

1 **Geochemical proxy systems in marine CaCO₃ biominerals record both** 2 **environmental changes and biomineralisation processes**

3
4 David Evans^{1*}, Rosalind E. M. Rickaby², Gavin L. Foster¹

5
6 ¹ School of Ocean and Earth Science, University of Southampton, UK

7 ² Department of Earth Sciences, University of Oxford, UK

8
9 *Corresponding author: d.evans@soton.ac.uk

10 11 **Abstract**

12 The isotopic and elemental composition of calcium carbonate formed by marine
13 organisms underpins a substantial portion of our knowledge of past climates. These
14 geochemical ‘proxy’ systems have revolutionised our understanding of
15 palaeoenvironmental change but remain largely rooted in empiricism because of
16 poorly understood biological ‘vital effects’. Here, we outline how this is both a
17 problem and an opportunity — while some proxies have their basis in biological
18 processes, this is the root cause of uncertainty in others. Moreover, integrating
19 geochemistry into biomineralisation models provides additional constraint on
20 cellular processes; geochemical data have untapped potential in the field of
21 biomineralisation and could be used to simultaneously understand the proxies in
22 question and to determine why biomineralising organisms are sensitive to
23 environmental change.

24
25 **KEYWORDS:** biomineralisation, trace element, stable isotope, ion transport, shell
26 chemistry, geochemical proxy, calcification

27 28 **INTRODUCTION**

29 *How has Earth’s surface environment changed since its formation?* The vastness of
30 geological time naturally leads us to this question, of central importance to
31 understanding how we, and the world around us, came to be. Notwithstanding
32 knowledge of relatively recent climatic change handed down through oral tradition,
33 the tools to unravel the enormous changes we now know to have taken place were
34 developed only in the mid-20th Century. Fast-forward to today and it seems
35 incredible to imagine a world in which this information did not exist; we now
36 understand that Earth’s climate has oscillated on temporal scales spanning many
37 orders of magnitude, from the hundred-million-year timescales of supercontinent
38 cycles to the subtle changes in Earth’s orbit around the Sun that paced geologically
39 recent glacial-interglacial climate change. Together, this knowledge not only puts
40 our present-day climate in context but also provides a valuable framing for the
41 interpretation of anthropogenic climate change (Lear et al. 2021). Of central
42 importance to this revolution in the natural sciences have been chemical analyses
43 of biologically formed calcium carbonate shells. In particular, since the mid-20th
44 Century, the chemical and isotopic composition of the shells and skeletons of a
45 diverse range of marine organisms, from tropical corals and edible molluscs through
46 to the tiny, single-celled foraminifera, have provided an enormous wealth of
47 information of Earth’s climatic evolution. Using these tools has, for example,

48 enabled us to reconstruct seasonality deep in the geological past, to determine how
49 polar ice sheets have waxed and waned through time, and perhaps of most crucial
50 societal importance, to benchmark climate model performance and constrain the
51 sensitivity of the Earth and climate system to changes in [the concentration of](#)
52 [atmospheric CO₂ in the atmosphere concentration](#).

53
54 Prior to the development of quantitative geochemical approaches, palaeoclimate
55 reconstructions were qualitative and based on comparisons to modern flora and
56 fauna. For example, the occurrence of tropical forests in the Eocene at mid-latitudes
57 was inferred from fossil vegetation assemblages. This changed with the discovery of
58 (stable) isotopes in the 1910s, which led to the pioneering work of Harold Urey on
59 the temperature-dependent fractionation of oxygen-18 relative to oxygen-16
60 between phases (Urey 1947) and resulted in the development of oxygen isotope
61 thermometry (Urey et al. 1951). This provided the first quantitative tool at our
62 disposal, which was soon followed by the characterisation of the relationship
63 between temperature and the incorporation of elemental impurities such as
64 magnesium into CaCO₃ (Chave 1954).

65
66 The intervening years have been characterised by the development of a wide range
67 of geochemical (trace) element 'proxy' systems in an ever-increasing number of
68 mineralising organisms across the phylogenetic tree. In large part, this has been
69 driven by technological developments, with the advent of inductively-coupled-
70 plasma optical emission spectroscopy in the 1950s followed by mass spectrometry
71 in the 1980s (ICPMS). Coevally, developments in gas-source mass spectrometers
72 mean that oxygen and carbon isotope measurements are now possible on samples
73 as small as the individual shells of single-celled calcifying plankton, while multi-
74 collector ICPMS instruments have opened up a suite of new stable isotope proxies.

75
76 These advances, together with experimental and theoretical evidence of the
77 behaviour of geochemical systems in abiotic ('inorganic') calcium carbonates, soon
78 led to the realisation that virtually all geochemical systems in biological-formed
79 carbonate are out of chemical equilibrium with the ambient seawater environment
80 in which these organisms live. For example, biogenic calcites are characterised by a
81 large degree of variability in terms of their magnesium content, ranging from
82 around 0-20 mol% MgCO₃, whereas inorganic calcite precipitated from seawater
83 contains ~8 mol% ([see e.g.](#) Branson et al. 2024). Likewise, the existence of
84 heterogeneity in CaCO₃ oxygen isotope data beyond that explicable by temperature
85 was known since the inception of the proxy (Urey et al. 1951, see Chen and Watkins,
86 this issue). This variability necessitates at the very least that some of these
87 minerals formed out of equilibrium with seawater, hinting at substantial biological or
88 disequilibrium imprints on shell chemistry. This phenomenon, often assigned the
89 catch-all term 'vital effect', is now known to impart some control on virtually every
90 biomineral based geochemical proxy system, and it is for this reason that the
91 overwhelming majority of proxy systems remain empirical and require the
92 assumption of uniformitarianism (the notion that Earth has always changed in
93 uniform ways and the present is the key to the past).

94

95 While such effects may be a nuisance for palaeoclimatologists, vital effects also
96 offer an opportunity: they tell us something about the biological process of
97 calcification. Using the above example, we might infer that an organism such as a
98 coccolithophore (single-celled photosynthesising algae), which produces trace metal
99 pure calcite, either transports calcium into, or magnesium out of, the calcification
100 site, effectively diluting the large amount of Mg present in seawater. Shell
101 geochemistry therefore not only provides a key source of palaeoclimatic information
102 but also offers important insight into how organisms build their shells, of key
103 relevance to understanding their sensitivity to climate change.

104

105 **GEOCHEMICAL WINDOWS INTO EARTH'S PAST ENVIRONMENTS**

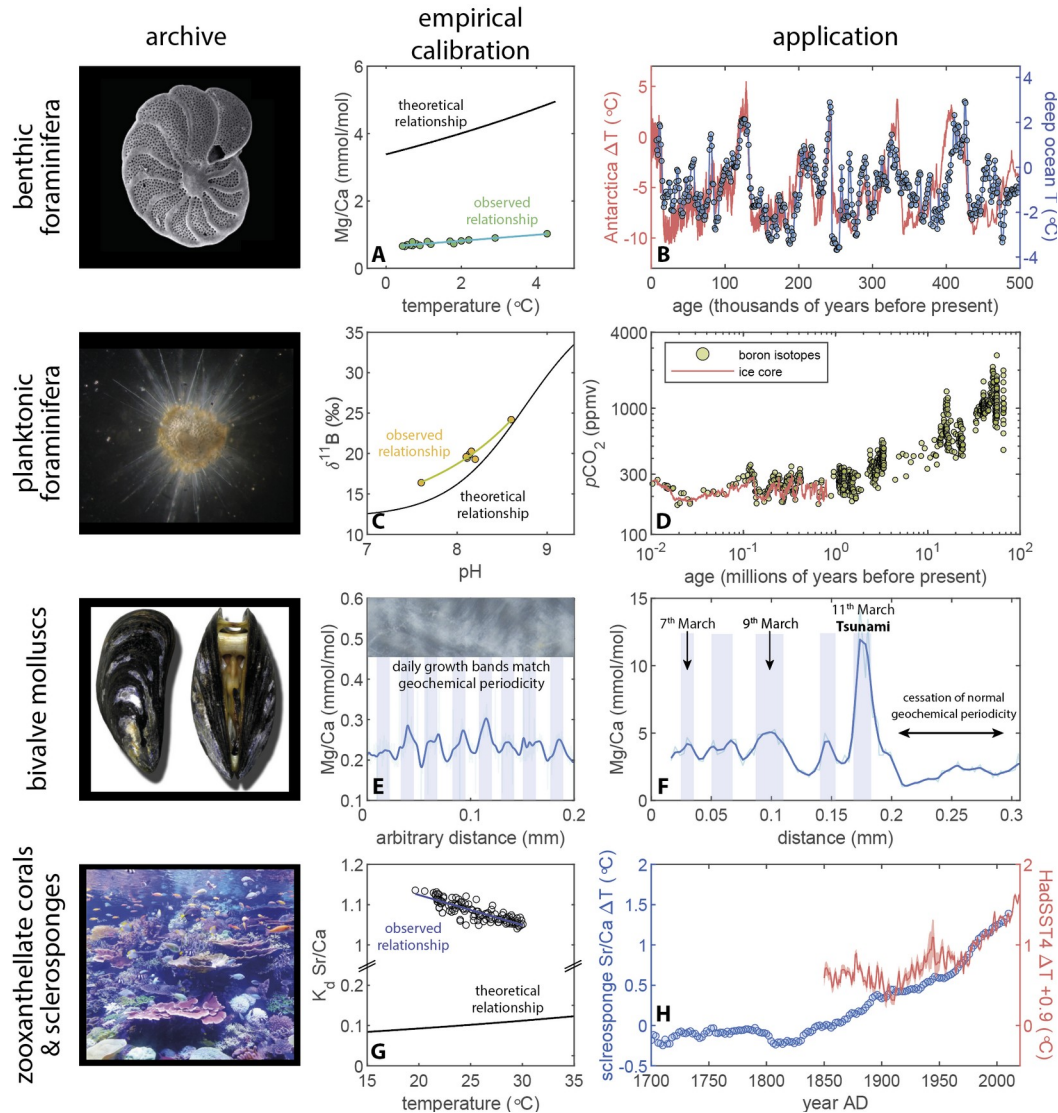
106 The vast wealth of proxies now available prevents us from providing a
107 comprehensive overview here. We therefore focus on four examples that give a
108 sense of the possibilities that await prospective palaeoclimatologists (Fig. 1). In
109 each case we briefly introduce the proxy system and explore how the system differs
110 from thermodynamic expectation.

111

112 ***Mg/Ca and Temperature reconstruction using Mg/Ca***

113 The dependency of the Mg/Ca ratio on temperature in the calcitic shells of
114 foraminifera has been utilised in both benthic and planktonic species and applied in
115 all ocean basins on Earth. Deep sea-dwelling species have notably been used to
116 determine temperature change in the deep ocean throughout the late Pleistocene
117 glacial cycles (Elderfield et al., 2012) and across the Cenozoic (Lear et al. 2000), in
118 the former case demonstrating a striking coherence with an entirely independent
119 record of Antarctic temperature change (Fig. 1B). The presence of foraminifera in
120 ocean sediment cores spanning the last ~100 million years thus offers the potential
121 to precisely reconstruct temperature change across geologic timescales. The proxy
122 is rooted in the thermodynamically controlled substitution of Mg for Ca in the calcite
123 crystal lattice, yet the enthalpy of the reaction predicts that this temperature
124 dependency of Mg incorporation should be substantially less sensitive than is
125 commonly observed in biogenic minerals. In addition, most species of foraminifera
126 are characterised by shell Mg/Ca many times lower than inorganic calcite
127 precipitated from seawater. Together, these comparisons (Fig. 1A) strongly suggest
128 that Mg is removed or Ca concentrated at the calcification site, with both processes
129 promoting calcification via the removal of a kinetic inhibitor or increasing saturation
130 state, respectively. While this means that all Mg/Ca-temperature calibrations are
131 empirical, this feature of shell chemistry has been enormously advantageous in that
132 the steeper empirical slope reduces the uncertainty in the resulting
133 palaeoenvironmental reconstructions. The corollary is that determining whether
134 there was an evolving biological control on this aspect of the biomineralisation
135 pathway is key to its accurate application across geologic time.

136



137
138

139 **FIGURE 1** Examples of geochemical proxy systems and their application, highlighting the
 140 empirical nature of quantification or calibration (note the offsets between the theoretical and
 141 observed proxy relationships). **(A)** Mg/Ca-temperature relationship in the shells of benthic
 142 foraminifera, applied **(B)** to reconstruct late-Pleistocene deep ocean temperature at ODP Site
 143 1123 (Elderfield et al. 2012), compared to the Antarctic ice core record. **(C)** The relationship
 144 between the boron isotopic composition of planktonic foraminifera and pH, applied **(D)**
 145 to reconstruct Cenozoic $p\text{CO}_2$ (pH and CO_2 are tightly coupled; Rae et al. 2021), compared to
 146 measurements from the composite Antarctic ice core record. **(E)** Daily growth bands visible
 147 in some mollusc shells (inset light microscope image) demonstrate daily geochemical
 148 periodicity in Mg/Ca (Arndt et al. 2023), applied **(F)** to identify the impact of the 2011
 149 Tōhoku tsunami on mollusc calcification (Sano et al. 2021), note the atypical size of the
 150 Mg/Ca peak and subsequent interruption of normal biomineralisation processes as the daily
 151 bands disappear. **(G)** The relationship between Sr/Ca and temperature in biogenic aragonite,
 152 applied **(H)** to extend the record of anthropogenic climate change beyond the instrumental
 153 record (McCulloch et al. 2024); HadSST4 data set (+0.9°C to align the two)), indicating that -
 154 at least in the Caribbean - 1.5°C global warming may already have occurred.

155 **Boron Isotopes, Ocean pH, and Atmospheric CO₂**

156 The boron isotopic composition of CaCO_3 ($\delta^{11}\text{B}$ [defined as the per mil deviation of
157 $^{11}\text{B}/^{10}\text{B}$ of a given sample from that of reference material NIST SRM 951]; see Chalk
158 and Rollion-Bard, this issue) records the pH of the aqueous solution from which it
159 formed with a well-understood mechanistic basis: two major species of boron are
160 present in seawater (borate and boric acid), ~~with~~ their proportions depend~~ant~~ on
161 pH. Because there is a large difference in the isotopic composition of the two
162 species, and borate is dominantly incorporated into CaCO_3 , $\delta^{11}\text{B}$ of boron trapped in
163 the mineral broadly records pH at the site of mineralisation. The pH of seawater is
164 closely tied to the concentration of CO_2 in the atmosphere (Rae et al. 2021), ~~such~~
165 ~~thate~~ much of our knowledge of past atmospheric CO_2 is derived from $\delta^{11}\text{B}$
166 measured in the sub-millimetre-sized planktonic foraminifera (Fig. 1D; e.g. Rae et al.
167 2021). The consistency of the $\delta^{11}\text{B}$ atmospheric CO_2 reconstructions with direct ice
168 core CO_2 measurements demonstrates the accuracy of the approach (de la Vega et
169 al. 2023). Building on this confidence, the $\delta^{11}\text{B}$ - CO_2 record now covers most of the
170 geological interval since the extinction of the dinosaurs. Like Mg/Ca-derived
171 palaeotemperatures, these reconstructions are based on empirical calibrations, as
172 most species do not form shells with the $\delta^{11}\text{B}$ ~~exactly the same as~~ seawater borate
173 (Fig. 1C). This suggests that foraminifera modify the pH of seawater from which they
174 calcify. In the example shown in FIGURE 1C, this may suggest an elevated
175 calcification site pH, which the organism may effect to aid calcite precipitation.
176 Given that calcification site pH is likely to be sensitive to ambient seawater pH in
177 many cases (this is one key reason that many calcifying organisms are sensitive to
178 ocean acidification), this provides an example of how a proxy system
179 simultaneously tells us something about the biomineralisation process of the
180 organism as well as the environment in which it lived.

181

182 **Daily Chemical Cyclicality in Growth-Banded Organisms**

183 Daily-resolution geochemical bands are present in many bivalve molluscs, such as
184 giant clams (*Tridacna*) and the edible mussel *Mytilus edulis* (Fig. 1E) which produce
185 continuously secreted layered shells. Laser microsampling of this banding has
186 revealed the presence of daily cyclicality in the concentrations of several trace
187 elements, which are demonstrably physiologically driven given that they are also
188 present in specimens grown under invariant laboratory conditions (Arndt et al. 2023
189 and references therein). The ability to count geochemical layering means that sub-
190 daily-resolved records of environmental conditions are possible in samples millions
191 of years old. The potential of this information is highlighted by the identification of a
192 known tsunami event in the shell of a mussel (Fig. 1F; Sano et al. 2021), ~~possible-~~
193 ~~because observed textural and geochemical bands can be counted backwards from-~~
194 ~~the day the specimen was sampled~~ visible as a stress-induced change in shell
195 chemistry, enabling shell geochemistry to be placed on an absolute chronology. This
196 case study highlights that mollusc shell geochemistry is controlled to a substantial
197 degree by the organism and thus provides an example of a proxy that has its basis
198 in circadian physiological processes which impact ion transport to the calcification
199 site. In the example shown in FIGURE 1F, the tsunami first resulted in a high-Mg/Ca
200 band, which is probably a stress-related response impacting the selectivity of
201 calcium versus magnesium transport (Sano et al. 2021), followed by a cessation of
202 banding as the circadian rhythm of the organism was interrupted.

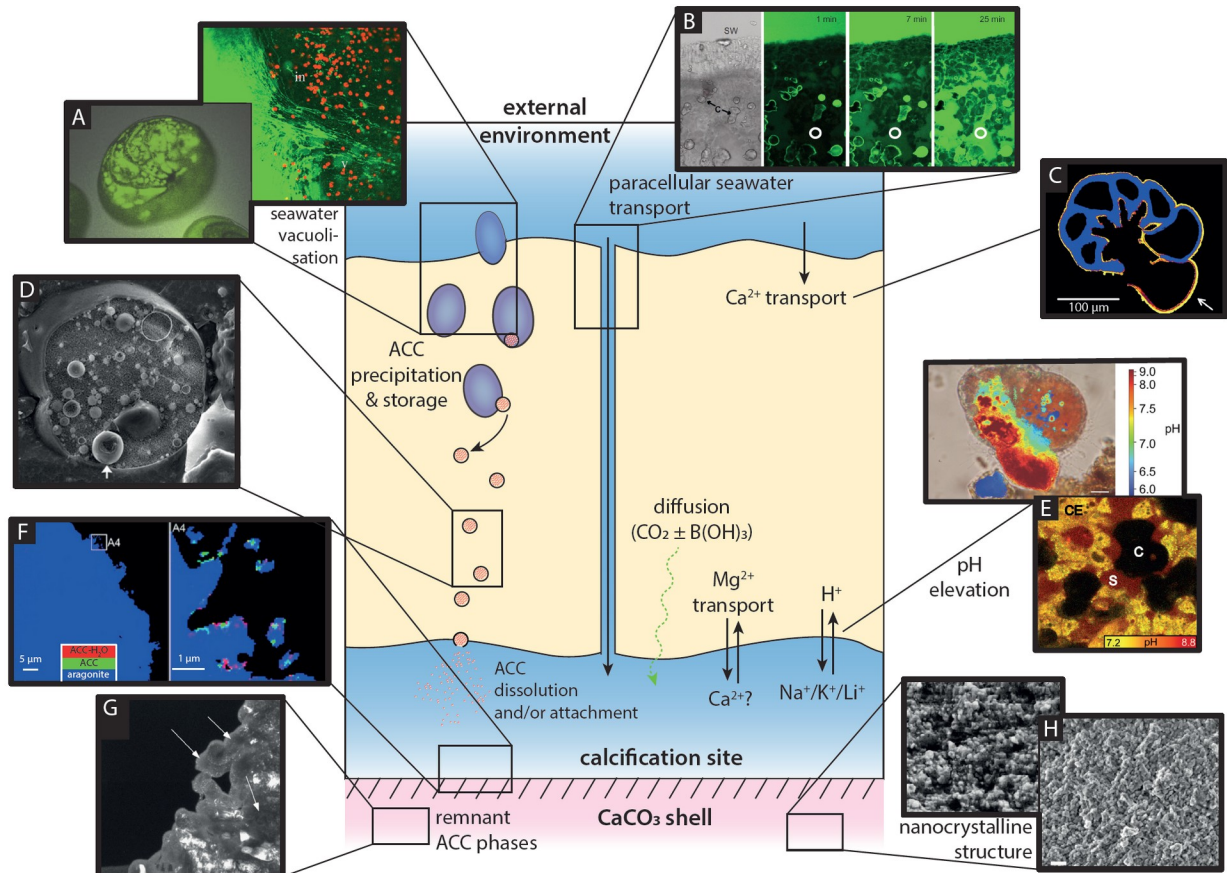
203
204
205
206
207
208
209
210
211
212
213
214
215
216
217
218
219
220
221
222
223
224
225
226
227
228
229
230
231
232
233
234
235
236
237
238
239
240
241
242
243
244
245
246
247
248

Placing anthropogenic warming in context using Sr/Ca thermometry

The strontium/calcium ratio (Sr/Ca) of coral and sclerosponge aragonite has been widely applied as a palaeothermometer and has found particular utility in unravelling recent (anthropogenic) climate change because many species produce regular growth bands which can be used to generate an absolute timescale. An example of this is shown in FIGURE 1H (McCulloch et al. 2024), in which sclerosponge Sr/Ca was used to show that substantial global warming occurred prior to the early 20th Century instrumental baseline, such that, at least in the Caribbean, the 1.5°C global warming target may already have been exceeded. Reconstructions such as this are based on empirical Sr/Ca-temperature calibrations, which differ from thermodynamic prediction in both the direction of change and degree of Sr substitution into the lattice (Fig. 1G; Gaetani and Cohen 2006). However, given that inorganic aragonite Sr/Ca similarly does not fit thermodynamic expectation (Gaetani and Cohen 2006), this offset cannot be purely physiologically driven. These observations suggest that the formation of both inorganic and biogenic aragonites take place a long way from equilibrium conditions, and are reconcilable with a model centred on the temperature-dependent entrapment and diffusion of ions in the poorly-ordered surface layer of a growing crystal (Watson 2004). This provides an example of an indirect biological control on a proxy system via the creation of conditions at the growing mineral surface which means that kinetic processes dominate, as opposed to the more direct control exerted via, for example, selective ion transport. Indeed, this may be the root cause of many other geochemical offsets that are lumped-placed under the umbrella of vital effects.

VITAL EFFECTS

The above examples highlight the wealth of societally and scientifically important insights that geochemical proxies have provided, from CO₂ changes deep in Earth's geologic past to determining the magnitude and onset of anthropogenic warming. In each case, the desired information was derived from empirical calibrations, with the differences between these and thermodynamic predictions or abiotic CaCO₃ illuminating some biological processes that alter the chemical composition at the calcification site from that of ambient seawater. For example, preferential inward transport of Ca, or outward transport of Mg (Branson and de Nooijer, this issue) and an elevation of calcification site pH (increasing the CaCO₃ saturation state by shifting inorganic carbon speciation from HCO₃⁻ to CO₃²⁻) both promote precipitation *and* alter the chemistry of the calcification site. A more comprehensive (albeit non-exhaustive) overview of the range of processes that may contribute to differences between biogenic and abiotic CaCO₃ chemistry are introduced in turn below within the context of a schematic model of biomineralisation (Fig. 2). This model and the overlain processes are not intended to represent a specific organism, but rather give an overview of the range of factors that cross disciplinary boundaries, and which could contribute to vital effects.



249
 250 **FIGURE 2** Schematic overview of biomineralisation processes that may fractionate the
 251 geochemistry of marine carbonate biominerals, with key supporting observations. No
 252 specific organism is represented; not all processes depicted here are applicable to all
 253 organisms. The ions for biomineralisation may be transported either as packages (vacuoles)
 254 of seawater (**A**: fluorescent confocal microscope image of calcein-labelled seawater (green-
 255 colour) ingressing into a high-Mg foraminifera, (Bentov et al. 2009; Evans et al. 2018; in =
 256 intracellular, v = vacuoles); red fluorescence results from symbiont autofluorescence) which
 257 may also 'leak' between cells (**B**): 'paracellular' seawater transport in corals (Venn et al.
 258 2020) timelapse fluorescent confocal images show labelled seawater permeating into the
 259 organism through time). Images in panels A and B track these processes using fluorescent
 260 membrane-impermeable labels placed into the seawater. Alternatively, the ions for
 261 calcification may be transported directly into the cell via membrane channels or pumps (**C**:
 262 isotope tracer evidence in a low-Mg foraminifer (Nehrke et al. 2013), in which it was shown
 263 that transfer of the organism to isotopically labelled seawater immediately before chamber
 264 formation resulted in an isotopically-labelled chamber, natural/spike Ca isotope ratio shown
 265 in blue and yellow respectively). Calcium (and carbon) may be stored intracellularly as
 266 amorphous calcium carbonate (ACC) before it is required (**D**: ACC spheres in sea urchin cells
 267 (Vidavsky et al. 2016) imaged using cryo-scanning electron microscopy). At the calcification
 268 site, pH may be raised (**E**: as evidenced by fluorescent confocal microscope imaging of pH-
 269 sensitive labels in foraminifera and corals (de Nooijer et al. 2009; Venn et al. 2011); CE =
 270 calcicoblastic epithelium, C = crystal, S = fluid filled space) in order to promote calcification,
 271 while calcium may be pumped in and Mg pumped out to achieve the same goal (**D**). In some
 272 organisms, delivery or precipitation of ACC to/at the calcification site has been observed (**F**:
 273 applying synchrotron photoemission electron microscopy to corals (Sun et al. 2020)) and
 274 remnant amorphous phases have been observed in the shell (**G**: darkfield transmission

275 electron microscopy image of a bivalve (Jacob et al. 2011), with crystalline material shown in
276 white while amorphous material that does not diffract appears dark, see arrows). Finally, the
277 nanogranular shell texture of a diverse range of biogenic carbonates may indicate
278 precipitation via an amorphous phase (**H**: scanning electron microscopy of fractured
279 surfaces of a planktonic foraminifer chamber wall and coral skeleton (Arns et al. 2022; Mor
280 Khalifa et al. 2021; images are $\sim 2 \mu\text{m}$ in diameter)).

281

282 Vital effects exist because calcification in all organisms takes place in a (semi)
283 enclosed space which has a composition that the organism modifies or controls. In
284 many cases, such as in the foraminifera and corals (Erez 2003; Venn et al. 2020),
285 the fluid's original composition in this space has been shown, or argued, to be
286 predominantly that of seawater, although this is probably not always the case, for
287 example in coccolithophores.

288

289 Seawater may be transported to the calcification site either via the process of
290 endocytosis, in which vacuoles (packages) of seawater are enclosed by a membrane
291 (Fig. 2A), or by leaking between cells (paracellular transport; Fig. 2B). Both
292 processes have been demonstrated by observing the transport of membrane-
293 impermeable fluorescent molecules to the calcification site (Erez 2003; Venn et al.
294 2020). In the former case the composition of the seawater may be modified and/or
295 precipitation of CaCO_3 may already take place before delivery to the calcification
296 site. This intracellular formation of CaCO_3 , particularly in an amorphous form that
297 readily facilitates its reuse (Fig. 2C; Jantschke and Scholz, this issue), may be a
298 useful strategy as it enables the rates of ion accumulation and shell or skeleton
299 formation to be decoupled, at which time some organisms might be particularly
300 vulnerable. The formation of an amorphous calcium carbonate (ACC) precursor
301 phase has potentially large ramifications for shell chemistry because ACC has a very
302 different elemental composition compared to crystalline CaCO_3 (Evans et al. 2020).

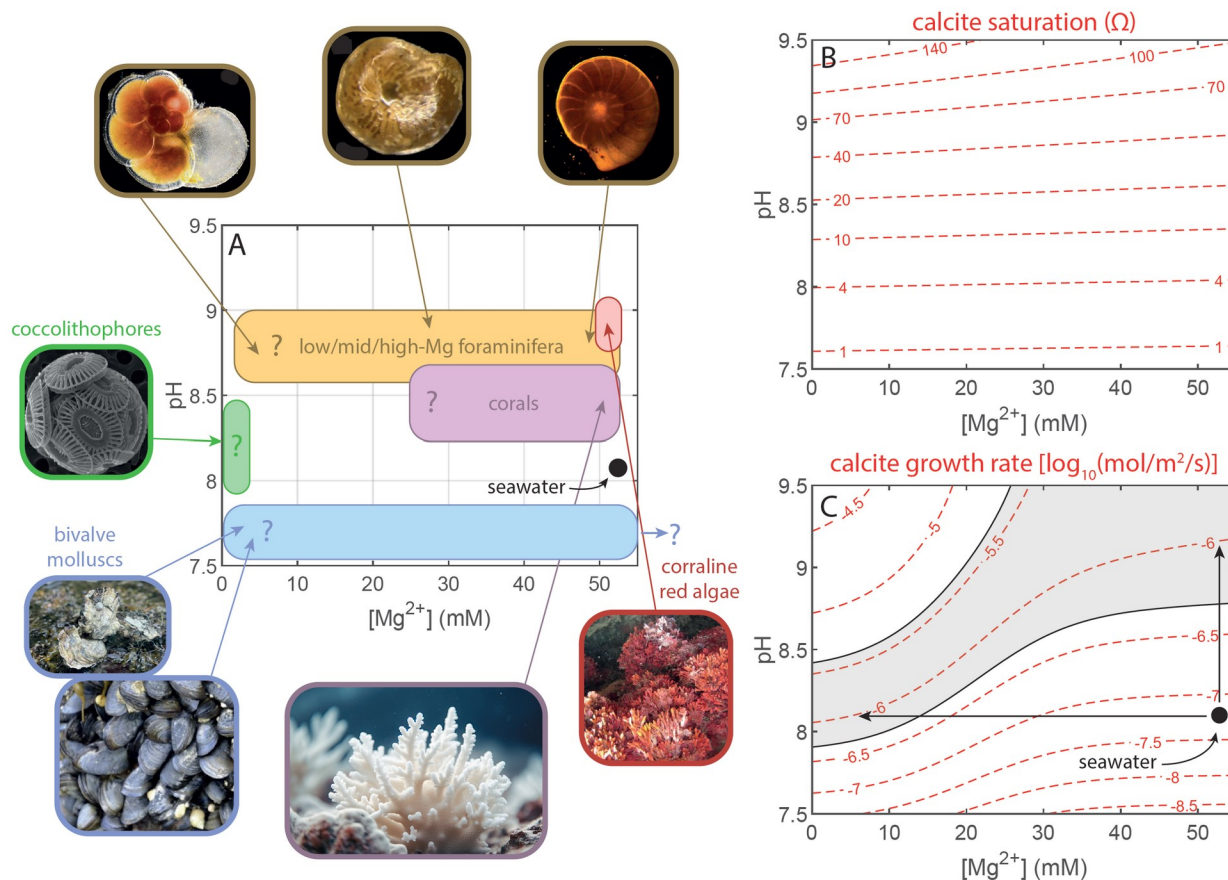
303

304 Alternatively, some organisms, such as the coccolithophores and certain species of
305 foraminifera, dominantly acquire the Ca^{2+} necessary for calcification via ion
306 transport, which has been argued for on the basis that some organisms do not
307 incorporate membrane-impermeable dyes, or rapidly acquire the composition of
308 isotopically labelled seawater (Fig. 2D; Nehrke et al. 2013). In this endmember case,
309 the composition of the calcification site will be determined by the selectivity of
310 channels and pumps for Ca over other elements present in seawater and the cytosol
311 (one of the liquids found inside cells).

312

313 The chemistry of the calcification site itself may be (further) modified. Outward
314 transport of magnesium favours precipitation as it has a 'poisoning' effect on CaCO_3
315 growth (Stolarski et al., this issue), which may be charge-balanced via the inward
316 delivery of calcium, acting to additionally increase saturation state. Simultaneously,
317 pH elevation, which has been demonstrated in foraminifera and corals (Fig. 2E; de
318 Nooijer et al. 2009; Venn et al. 2011), aids precipitation by increasing the
319 $\text{CO}_3^{2-}/\text{HCO}_3^-$ ratio and promoting inward CO_2 diffusion (Chen and Watkins, this issue),
320 helping to provide carbon necessary for calcification. These processes influence

321 trace element thermometers, stable isotope compositions, and boron isotope
 322 systematics, as described above.



323
 324
 325 **FIGURE 3.** An example of two strategies to facilitate calcium carbonate precipitation from
 326 seawater: increasing pH (vertical axis) or removing Mg^{2+} (horizontal axis). The former
 327 increases the saturation state of seawater by shifting carbon speciation towards CO_3^{2-} and
 328 potentially increases the concentration of dissolved inorganic carbon (DIC) by promoting
 329 inwards diffusion of CO_2 , while the latter reduces the inhibitory effect of Mg^{2+} on $CaCO_3$
 330 crystal growth. **(A)** The possible calcification site conditions of diverse marine calcifying
 331 organisms. We stress that this is an indicative guide only, with the location of some fields
 332 highly uncertain and inferred in many cases from shell chemistry. **(B)** The impact of pH and
 333 $[Mg^{2+}]$ on seawater calcite saturation index (Ω), derived with the PHREEQC geochemical
 334 model PHREEQC. To model the effect of pH elevation on CO_2 diffusion, this example
 335 calculation covaries pH and DIC (see the supplementary materials for details). Contours of
 336 saturation index (dashed) are broadly horizontal because $[Mg^{2+}]$ has little effect on the
 337 activities of Ca^{2+} and CO_3^{2-} activities. **(C)** The effect of pH/DIC and $[Mg^{2+}]$ on the rate of
 338 calcite crystal growth based on empirical growth rate equations (see the supplementary
 339 materials). Contours of growth rate (dashed) are sigmoidal in contrast to panel **B** because
 340 Mg^{2+} inhibits crystal growth. The shaded region shows estimated growth rates of
 341 foraminifera (see Branson et al. 2024 and references therein), shown as an example as an
 342 empirical estimate of surface area normalised precipitation rate are is available for this
 343 organism. Starting from normal seawater, two strategies to increase precipitation rate are
 344 apparent (arrows).
 345

346 Finally, the delivery of ACC in some biomineralising organisms may modify
347 shell/skeletal chemistry either indirectly, by changing the composition of the
348 calcification site if [the ACC](#) dissolves, or directly, via attachment to the growing
349 crystal surface (Fig. 2F). Remnant amorphous phases observed in the shells of some
350 organisms (Fig. 2G) and the nanocrystalline structure of many biominerals (Fig. 2H)
351 provide evidence for this. The degree to which this process controls mineral
352 chemistry depends on the transformation mechanism(s), specifically, whether ACC
353 dissolves and reprecipitates as a carbonate mineral or if it reorders in the solid
354 state. To our knowledge, this distinction (or the relative importance of the two
355 paths) remains unknown for any system of interest and is thus a major source of
356 uncertainty in terms of understanding the mechanistic basis of proxy systems.

357
358 The above description of biological processes that deliver ions to the calcification
359 site and promote precipitation leads us to the question: *what are the evolutionary*
360 *benefits of opting one process over another?* To provide one answer and to highlight
361 the applicability of geochemical data to understanding biomineralisation processes,
362 we use the case study of the impact that Mg^{2+} and pH have on $CaCO_3$ precipitation,
363 following Zeebe and Sanyal (2002). Increasing pH shifts carbon speciation towards
364 CO_3^{2-} and therefore increases the $CaCO_3$ saturation state ($\Omega = [Ca^{2+}][CO_3^{2-}]/K_{sp}^*$,
365 where K_{sp}^* is the stoichiometric solubility product and square brackets denote
366 concentration), thus facilitating calcification and promoting inwards diffusion of CO_2 .
367 In contrast, changing $[Mg^{2+}]$ has a very minor impact on Ω . However, several marine
368 calcifying phyla (e.g. molluscs, some foraminifera, and coccolithophores) produce
369 calcite with Mg/Ca that is so much lower than inorganic calcite that it presumably
370 must imply large degrees of ion transport to lower the calcification site Mg/Ca. The
371 likely reason for this is that the presence of Mg^{2+} in solution inhibits $CaCO_3$ growth
372 because the removal of the Mg^{2+} hydration sphere on attachment is a slow process
373 relative to that of Ca^{2+} (seawater Mg/Ca = ~ 5). As such, while Mg has little impact
374 on the degree of oversaturation (Fig. 3B), solutions with higher Mg/Ca kinetically
375 favour the precipitation of the more soluble $CaCO_3$ polymorph aragonite, or they
376 lower the rates of calcite precipitation where that polymorph can be engineered. To
377 illustrate this, we show the empirical impact of pH and $[Mg^{2+}]$ on the growth rate of
378 inorganic calcite (Fig. 3C), calculated using growth rate data sets (combining those
379 of Nielsen et al. 2016, and Wolthers et al. 2012). Doing so results in sigmoidal
380 growth rate isopleths (cf. Fig 3B), illustrating that raising the pH by ~ 1 unit, or
381 removing almost all of the Mg from seawater, increases in calcite precipitation rate
382 by around an order of magnitude in both cases.

383
384 This exercise demonstrates that both processes (pH increase and Mg^{2+} removal)
385 greatly aid rapid shell or skeleton formation and are likely to be a key reason for
386 selective ion transport and pH elevation. It is interesting to note that different
387 marine organisms sit in very different regions of this $[Mg^{2+}]$ -pH space (Fig. 3A), with
388 some possibly opting exclusively to raise pH or decrease $[Mg^{2+}]$. Given that Mg
389 transport is almost certainly more energetically costly than pH elevation (Zeebe and
390 Sanyal 2002), that some organisms employ this pathway implies that shell
391 precipitation rate is not the only factor 'being optimised'; e.g. the structural

392 properties of the resulting biomineral, or modifying Mg/Ca in order to preferentially
393 form calcite over aragonite, may be worth the energetic cost of ion transport.

394

395 **CONCLUDING REMARKS - A PROBLEM AND AN OPPORTUNITY**

396 Above, we briefly explore the variety of reasons that biological calcification yields a
397 shell or skeleton that differs compositionally in chemical or (and) isotopic-
398 composition terms from thermodynamic expectations and (or) abiotic CaCO₃. While
399 this complicates proxies, in that no system has a fully understood mechanistic basis,
400 many systems would be far less useful for environmental reconstructions without
401 their biological overprints. For example, Mg²⁺ incorporation in planktonic
402 foraminifera is three times more sensitive to temperature than in inorganic calcite,
403 diurnal geochemical banding would not exist if calcification were not tightly
404 mediated in molluscs (Fig. 1E), and the boron isotopic composition of aragonitic
405 skeletons may simultaneously record calcification site and seawater pH, given that
406 the two are often tightly linked.

407

408 Moreover, vital effects afford us the opportunity of simultaneously understanding
409 both biomineralisation processes and past environmental changes. The co-evolution
410 of shell mineralogy and seawater major element chemistry provides insight into the
411 effect that an organism's environment has on its calcification pathway (Stolarski et
412 al., this issue). More broadly, shell geochemistry is a valuable tool to understand
413 biomineralisation processes because the observations are noninvasive given that
414 they can be made on the skeletal material left after the organism has died, although
415 direct observations of biophysical processes are, of course, also essential. The
416 measurement of multiple different chemical systems coupled with an ever-improved
417 understanding of their behaviour in comparative abiotic experiments mean that we
418 stand at a transformative time in the application of shell chemistry to the study of
419 biomineralisation. Given that mechanistically understanding calcification processes
420 is key to improving proxy-derived palaeoenvironmental reconstructions by moving
421 these beyond purely empirical approaches, this knowledge will greatly benefit both
422 fields ~~greatly~~, which in turn, should be more closely integrated: the copious proxy
423 data that were generated primarily or initially for the purposes of climate research
424 remain largely untapped in constraining biomineralisation processes, for example.

425

426 In this issue, the subsequent articles give specific examples of how this may be
427 achieved, while providing overviews and details of the key proxy systems and
428 biomineralisation processes (Fig. 2). Our aim is that this contribution be used as a
429 springboard towards ensuring that geochemical proxies are fully leveraged in
430 informing biomineralisation models, and that direct observations of
431 biomineralisation processes are used to mechanistically understand proxies.
432 Ultimately, both fields will benefit from being more closely connected.

433

434 **ACKNOWLEDGMENTS**

435 GLF wishes to acknowledge support from the ERC grant number #884650. RR
436 acknowledges support from European Research Council (ERC) under the European Union's
437 Horizon 2020 research and innovation program (SCOOBI project, grant agreement no.
438 101019146; RER) and from the Natural Environment Research Council (NERC; PUCCA

439 project, award NE/V011049/1; RER). DE acknowledges support from the Royal Society
440 (award reference URF\R1\221735) and is greatly indebted to Jonathan Erez for our many
441 inspiring conversations over 'mud coffee', without which this issue would not have been
442 proposed. We would like to express our sincere thanks to the principal editors (Janne
443 Blichert-Toft and Tom Sisson) and two reviewers (James Rae and Michael Henehan) for
444 providing thoughtful comments that greatly improved this contribution.

445
446

REFERENCES

- 447 Arndt, I., Coenen, D., Evans, D., Renema, W., Müller, W., 2023. Quantifying Sub-Seasonal
448 Growth Rate Changes in Fossil Giant Clams Using Wavelet Transformation of Daily Mg/
449 Ca Cycles. *Geochemistry, Geophysics, Geosystems* 24, e2023GC010992.
450 <https://doi.org/10.1029/2023GC010992>
- 451 Arns, A.I., Evans, D., Schiebel, R., Fink, L., Mezger, M., Alig, E., Linckens, J., Jochum, K.P.,
452 Schmidt, M.U., Jantschke, A., Haug, G.H., 2022. Mesocrystalline Architecture in
453 Hyaline Foraminifer Shells Indicates a Non-Classical Crystallisation Pathway.
454 *Geochemistry, Geophysics, Geosystems* 23, e2022GC010445.
455 <https://doi.org/10.1029/2022GC010445>
- 456 Bentov, S., Brownlee, C., Erez, J., 2009. The role of seawater endocytosis in the
457 biomineralization process in calcareous foraminifera. *PNAS* 106, 21500–21504.
458 <https://doi.org/10.1073/pnas.0906636106>
- 459 Branson, O., Chauhan, N., Evans, D., Foster, G., Rickaby, R., 2024. Geochemical tracers of
460 biomineralisation processes, in: *Treatise on Geochemistry*.
- 461 Chave, K.E., 1954. Aspects of the Biogeochemistry of Magnesium 1. *Calcareous Marine*
462 *Organisms. The Journal of Geology* 62, 266–283. <https://doi.org/10.1086/626162>
- 463 de la Vega, E., Chalk, T.B., Hain, M.P., Wilding, M.R., Casey, D., Gledhill, R., Luo, C., Wilson,
464 P.A., Foster, G.L., 2023. Orbital CO₂ reconstruction using boron isotopes during the
465 late Pleistocene, an assessment of accuracy. *Climate of the Past* 19, 2493–2510.
466 <https://doi.org/10.5194/cp-19-2493-2023>
- 467 de Nooijer, L.J., Toyofuku, T., Kitazato, H., 2009. Foraminifera promote calcification by
468 elevating their intracellular pH. *PNAS* 106, 15374–15378.
469 <https://doi.org/10.1073/pnas.0904306106>
- 470 Elderfield, H., Ferretti, P., Greaves, M., Crowhurst, S., McCave, I.N., Hodell, D., Piotrowski,
471 A.M., 2012. Evolution of Ocean Temperature and Ice Volume Through the Mid-
472 Pleistocene Climate Transition. *Science* 337, 704–709.
473 <https://doi.org/10.1126/science.1221294>
- 474 Erez, J., 2003. The Source of Ions for Biomineralization in Foraminifera and Their Implications
475 for Paleooceanographic Proxies. *Reviews in Mineralogy and Geochemistry* 54, 115–149.
476 <https://doi.org/10.2113/0540115>
- 477 Evans, D., Gray, W.R., Rae, J.W.B., Greenop, R., Webb, P.B., Penkman, K., Kröger, R., Allison,
478 N., 2020. Trace and major element incorporation into amorphous calcium carbonate
479 (ACC) precipitated from seawater. *Geochimica et Cosmochimica Acta* 290, 293–311.
480 <https://doi.org/10.1016/j.gca.2020.08.034>
- 481 Evans, D., Müller, W., Erez, J., 2018. Assessing foraminifera biomineralisation models through
482 trace element data of cultures under variable seawater chemistry. *Geochimica et*
483 *Cosmochimica Acta, Chemistry of oceans past and present: A Special Issue in tribute*
484 *to Harry Elderfield* 236, 198–217. <https://doi.org/10.1016/j.gca.2018.02.048>
- 485 Gaetani, G.A., Cohen, A.L., 2006. Element partitioning during precipitation of aragonite from
486 seawater: A framework for understanding paleoproxies. *Geochimica et Cosmochimica*
487 *Acta* 70, 4617–4634. <https://doi.org/10.1016/j.gca.2006.07.008>
- 488 Jacob, D.E., Wirth, R., Soldati, A.L., Wehrmeister, U., Schreiber, A., 2011. Amorphous calcium
489 carbonate in the shells of adult *Unionoida*. *Journal of Structural Biology* 173, 241–249.
490 <https://doi.org/10.1016/j.jsb.2010.09.011>
- 491 Lear, C.H., Anand, P., Blenkinsop, T., Foster, G.L., Gagen, M., Hoogakker, B., Larter, R.D.,
492 Lunt, D.J., McCave, I.N., McClymont, E., Pancost, R.D., Rickaby, R.E.M., Schultz, D.M.,

493 Summerhayes, C., Williams, C.J.R., Zalasiewicz, J., 2021. Geological Society of London
494 Scientific Statement: what the geological record tells us about our present and future
495 climate. *Journal of the Geological Society* 178, jgs2020-239.
496 <https://doi.org/10.1144/jgs2020-239>

497 Lear, C.H., Elderfield, H., Wilson, P.A., 2000. Cenozoic Deep-Sea Temperatures and Global Ice
498 Volumes from Mg/Ca in Benthic Foraminiferal Calcite. *Science* 287, 269-272.
499 <https://doi.org/10.1126/science.287.5451.269>

500 McCulloch, M.T., Winter, A., Sherman, C.E., Trotter, J.A., 2024. 300 years of sclerosponge
501 thermometry shows global warming has exceeded 1.5 °C. *Nat. Clim. Chang.* 14, 171-
502 177. <https://doi.org/10.1038/s41558-023-01919-7>

503 Mor Khalifa, G., Levy, S., Mass, T., 2021. The calcifying interface in a stony coral primary
504 polyp: An interplay between seawater and an extracellular calcifying space. *Journal of*
505 *Structural Biology* 213, 107803. <https://doi.org/10.1016/j.jsb.2021.107803>

506 Nehrke, G., Keul, N., Langer, G., de Nooijer, L.J., Bijma, J., Meibom, A., 2013. A new model for
507 biomineralization and trace-element signatures of Foraminifera tests. *Biogeosciences*
508 10, 6759-6767. <https://doi.org/10.5194/bg-10-6759-2013>

509 Nielsen, M.R., Sand, K.K., Rodriguez-Blanco, J.D., Bovet, N., Generosi, J., Dalby, K.N., Stipp,
510 S.L.S., 2016. Inhibition of Calcite Growth: Combined Effects of Mg²⁺ and SO₄²⁻.
511 *Crystal Growth & Design* 16, 6199-6207. <https://doi.org/10.1021/acs.cgd.6b00536>

512 Rae, J.W.B., Zhang, Y.G., Liu, X., Foster, G.L., Stoll, H.M., Whiteford, R.D.M., 2021.
513 Atmospheric CO₂ over the Past 66 Million Years from Marine Archives. *Annual Review of*
514 *Earth and Planetary Sciences* 49, 609-641. <https://doi.org/10.1146/annurev-earth-082420-063026>

515 Sano, Y., Okumura, T., Murakami-Sugihara, N., Tanaka, K., Kagoshima, T., Ishida, A., Hori, M.,
516 Snyder, G.T., Takahata, N., Shirai, K., 2021. Influence of normal tide and the Great
517 Tsunami as recorded through hourly-resolution micro-analysis of a mussel shell. *Sci*
518 *Rep* 11, 19874. <https://doi.org/10.1038/s41598-021-99361-2>

519 Sun, C.-Y., Stiffler, C.A., Chopdekar, R.V., Schmidt, C.A., Parida, G., Schoeppler, V., Fordyce,
520 B.I., Brau, J.H., Mass, T., Tambutté, S., Gilbert, P.U.P.A., 2020. From particle attachment
521 to space-filling coral skeletons. *Proceedings of the National Academy of Sciences* 117,
522 30159-30170. <https://doi.org/10.1073/pnas.2012025117>

523 Urey, H., 1947. The thermodynamic properties of isotopic substances. *Journal of the*
524 *Chemical Society* 562-581.

525 Urey, H.C., Lowenstam, H.A., Epstein, S., McKinney, C.R., 1951. Measurement of
526 paleotemperatures and temperatures of the upper Cretaceous of England, Denmark,
527 and the southeastern United States. *GSA Bulletin* 62, 399-416.
528 [https://doi.org/10.1130/0016-7606\(1951\)62\[399:MOPATO\]2.0.CO;2](https://doi.org/10.1130/0016-7606(1951)62[399:MOPATO]2.0.CO;2)

529 Venn, A., Tambutté, E., Holcomb, M., Allemand, D., Tambutté, S., 2011. Live Tissue Imaging
530 Shows Reef Corals Elevate pH under Their Calcifying Tissue Relative to Seawater.
531 *PLOS ONE* 6, e20013. <https://doi.org/10.1371/journal.pone.0020013>

532 Venn, A.A., Bernardet, C., Chabenat, A., Tambutté, E., Tambutté, S., 2020. Paracellular
533 transport to the coral calcifying medium: effects of environmental parameters.
534 *Journal of Experimental Biology* 223, jeb227074. <https://doi.org/10.1242/jeb.227074>

535 Vidavsky, N., Addadi, S., Schertel, A., Ben-Ezra, D., Shpigel, M., Addadi, L., Weiner, S., 2016.
536 Calcium transport into the cells of the sea urchin larva in relation to spicule
537 formation. *Proceedings of the National Academy of Sciences* 113, 12637-12642.
538 <https://doi.org/10.1073/pnas.1612017113>

539 Watson, E.B., 2004. A conceptual model for near-surface kinetic controls on the trace-
540 element and stable isotope composition of abiogenic calcite crystals¹. *Geochimica et*
541 *Cosmochimica Acta* 68, 1473-1488. <https://doi.org/10.1016/j.gca.2003.10.003>

542 Wolthers, M., Nehrke, G., Gustafsson, J.P., Van Cappellen, P., 2012. Calcite growth kinetics:
543 Modeling the effect of solution stoichiometry. *Geochimica et Cosmochimica Acta* 77,
544 121-134. <https://doi.org/10.1016/j.gca.2011.11.003>

545

546 Zeebe, R.E., Sanyal, A., 2002. Comparison of two potential strategies of planktonic
547 foraminifera for house building: Mg²⁺ or H⁺ removal? *Geochimica et Cosmochimica*
548 *Acta* 66, 1159–1169. [https://doi.org/10.1016/S0016-7037\(01\)00852-3](https://doi.org/10.1016/S0016-7037(01)00852-3)
549